Brain Advance Access published May 16, 2015

doi:10.1093/brain/awv136 BRAIN 2015: Page 1 of 10 | 1

BRAIN
A JOURNAL OF NEUROLOGY

Longitudinal changes in free-water within the substantia nigra of Parkinson's disease

Edward Ofori,[1] Ofer Pasternak,[2] Peggy J. Planetta,[1] Hong Li,[3] Roxana G. Burciu,[1] Amy F. Snyder,[1] Song Lai,[4,5] Michael S. Okun[6,7] and David E. Vaillancourt[1,6,8]

There is a clear need to develop non-invasive markers of substantia nigra progression in Parkinson's disease. We previously found elevated free-water levels in the substantia nigra for patients with Parkinson's disease compared with controls in single-site and multi-site cohorts. Here, we test the hypotheses that free-water levels in the substantia nigra of Parkinson's disease increase following 1 year of progression, and that baseline free-water levels in the substantia nigra predict the change in bradykinesia following 1 year. We conducted a longitudinal study in controls ($n = 19$) and patients with Parkinson's disease ($n = 25$). Diffusion imaging and clinical data were collected at baseline and after 1 year. Free-water analyses were performed on diffusion imaging data using blinded, hand-drawn regions of interest in the posterior substantia nigra. A group effect indicated free-water values were increased in the posterior substantia nigra of patients with Parkinson's disease compared with controls ($P = 0.003$) and we observed a significant group × time interaction ($P < 0.05$). Free-water values increased for the Parkinson's disease group after 1 year ($P = 0.006$), whereas control free-water values did not change. Baseline free-water values predicted the 1 year change in bradykinesia scores ($r = 0.74$, $P < 0.001$) and 1 year change in Montreal Cognitive Assessment scores ($r = -0.44$, $P = 0.03$). Free-water in the posterior substantia nigra is elevated in Parkinson's disease, increases with progression of Parkinson's disease, and predicts subsequent changes in bradykinesia and cognitive status over 1 year. These findings demonstrate that free-water provides a potential non-invasive progression marker of the substantia nigra.

1 Department of Applied Physiology and Kinesiology, University of Florida, USA
2 Departments of Psychiatry and Radiology, Brigham and Women's Hospital, Harvard Medical School, USA
3 Department of Preventative Medicine, Rush University Medical Centre, USA
4 Department of Radiation Oncology, University of Florida, USA
5 Human Imaging Core, Clinical and Translational Science Institute, University of Florida, USA
6 Department of Neurology and Centre for Movement Disorders and Neurorestoration, University of Florida, USA
7 Departments of Neurosurgery, Psychiatry, and History, University of Florida, USA
8 Department of Biomedical Engineering, University of Florida, USA

Correspondence to: David Vaillancourt, PhD,
Professor of Applied Physiology and Kinesiology,
Biomedical Engineering and Neurology,
University of Florida,
PO Box 118205, USA
E-mail: vcourt@ufl.edu

Keywords: substantia nigra; Parkinson's disease; diffusion MRI; extracellular space; longitudinal

Abbreviations: MDS-UPDRS = Movement Disorders Society Unified Parkinson's Disease Rating Scale; MoCA = Montreal Cognitive Assessment

Received January 14, 2015. Revised March 16, 2015. Accepted March 23, 2015.

Introduction

Parkinson's disease is a progressive neurodegenerative disease that is characterized by the loss of dopaminergic cells in the substantia nigra. Neuronal degeneration of the substantia nigra is greatest around the ventrolateral tier (Fearnley and Lees, 1991; Kordower *et al.*, 2013) and progresses to the dorsomedial tier (Damier *et al.*, 1999). Several studies using diffusion MRI revealed changes in specific subregions of the substantia nigra in patients with Parkinson's disease when compared with healthy control subjects (Vaillancourt *et al.*, 2009; Péran *et al.*, 2010; Du *et al.*, 2011; Prodoehl *et al.*, 2013). These studies demonstrated an increase in the magnitude and a reduction in the directional dependence of water diffusion processes in the substantia nigra. Recently, a novel diffusion MRI analysis technique using a bi-tensor model was introduced allowing the estimation for the fractional volume of free-water within a voxel (Pasternak *et al.*, 2009). Free-water is water molecules that do not experience a directional dependence or other restrictions by the cellular environment (Pasternak *et al.*, 2009; Metzler-Baddeley *et al.*, 2012). As the diffusion time of most conventional diffusion MRI sequences are ~40 ms, free-water estimates spaces larger than a few tens of micrometres and likely represents the extracellular space (Wang *et al.*, 2011*b*; Pasternak *et al.*, 2012). Our group recently investigated whether the bi-tensor model detects changes in the substantia nigra using baseline data from large cohorts of patients with Parkinson's disease and control subjects at a single site and across a multi-site study. We found that free-water was elevated for Parkinson's disease compared with control subjects in the same posterior region of the substantia nigra in both the single-site and multi-site cohorts (Ofori *et al.*, 2015).

Despite the clear evidence for cross-sectional Parkinson's disease-related changes in the substantia nigra using diffusion MRI, few longitudinal studies exist (Rossi *et al.*, 2014), and none have examined how free-water measures in the substantia nigra change with Parkinson's disease progression. Here, we chose to study progression following 1 year because this is a desirable time-frame for most disease modifying clinical trials in Parkinson's disease. We examined two hypotheses. First, we tested the hypothesis that the posterior substantia nigra free-water levels in Parkinson's disease increase following 1 year, with no changes in a control group. Second, we tested the hypothesis that the baseline posterior substantia nigra free-water levels predict the subsequent 1 year change in bradykinesia. If confirmed, these findings would provide the first study to demonstrate that free-water analysis of diffusion imaging within the substantia nigra could be used to monitor progression of Parkinson's disease after 1 year, and predict subsequent changes in bradykinesia.

Materials and methods

Subjects

Forty-four subjects participated between 2011 and 2014 in the current study. Data from 19 healthy individuals and 25 patients with Parkinson's disease were collected over two visits separated by ~1 year [controls (mean ± standard deviation, SD), 13.3 months ± 1.7; Parkinson's disease, 13.6 months ± 1.4] (Table 1). Patients with Parkinson's disease were diagnosed by movement disorders specialists based on the UK Parkinson's Disease Society Brain Bank criteria (Hughes *et al.*, 2001). Patients with Parkinson's disease were referred from the University of Florida Centre for Movement Disorders and Neurorestoration, whereas control subjects were recruited from the local and surrounding communities in North Central Florida. All patients with Parkinson's disease were early stage patients with Hoehn-Yahr scores of either 1 or 2. Control subjects reported no history of neurological or psychiatric disease. Patients with Parkinson's disease were tested at ~11:00 am after an overnight withdrawal from

Table 1 Demographic and clinical information

	Healthy controls (n = 19)		Parkinson's patients (n = 25)				
	Baseline	Year 1	Baseline	Year 1	Group effect	Time effect	Interaction
Age, years (SD)	65.3 (10.1)	—	65.3 (9.1)	—	0.99	—	—
Sex, % female	47.4%	—	20%	—	0.054	—	—
Hand dominance, left:right	4:15	—	3:22	—	0.661	—	—
Disease duration, months (SD)	—	—	36.3 (17.8)	49.8 (17.7)	—	<0.001**	—
MDS-UPDRS part III	2.1 (1.7)	4.36 (3.2)	28.5 (10.2)	31.0 (10.5)	<0.001**	0.007**	0.889
Bradykinesia	0.6 (0.9)	1.9 (2.4)	12.2 (4.7)	15.7 (5.9)	<0.001**	<0.001**	0.05*
Rigidity	0.4 (0.6)	0.6 (0.9)	5.8 (4.0)	5.3 (3.8)	<0.001**	0.754	0.376
Tremor	1.0 (1.4)	1.4 (1.6)	6.4 (3.9)	6.4 (3.9)	<0.001**	0.682	0.683
Gait/posture	0.1 (0.2)	0 (0.0)	1.9 (1.8)	2.6 (2.3)	<0.001**	0.196	0.125
Hoehn and Yahr	—	—	1.9 (0.4)	2.0 (0.6)	—	>0.99	—
MoCA	26.9 (2.1)	27.3 (2.1)	25.5 (2.5)	25.1 (3.6)	0.023*	0.947	0.347
Beck Depression Inventory	4.2 (4.9)	4.0 (4.5)	8.3 (7.2)	8.6 (6.1)	0.012*	0.968	0.676

*P < 0.05, **P < 0.01.

parkinsonian medications. Table 2 lists Parkinsonian medications, usage, and half-lifes. Patients with Parkinson's disease were excluded if they were taking rasagiline. All subjects gave written informed consent, as approved by the local Institutional Review Board. Demographic and clinical characteristics, including disease severity based on the Movement Disorders Society Unified Parkinson's Disease Rating Scale (MDS-UPDRS) part III and global cognitive function as measured by the Montreal Cognitive Assessment (MoCA) were collected for Parkinson's disease and control participants. The total score from the motor section of the MDS-UPDRS III was broken down into subscales for bradykinesia, rigidity, tremor, and axial function/balance/gait according to previous studies (Prodoehl *et al.*, 2010; Goetz *et al.*, 2012). In addition, we administered the Beck Depression Inventory (Beck *et al.*, 1961) to all participants at both time points.

Diffusion MRI acquisition

Diffusion-weighted images were acquired on a 3 T Philips Medical Systems MRI scanner (Achieva) using a 32-channel head coil at the McKnight Brain Institute. The Philips 3 T used in the current study met routine quality assurance. Also, previous work demonstrates reproducible substantia nigra free-water elevation in Parkinson's disease across single- and multi-site studies suggesting that increased free-water can be detected in Parkinson's disease despite inherent differences across sites.

Whole brain diffusion imaging data were acquired using a single-shot spin echo EPI sequence, and the sequence consisted of the following parameters: repetition time = 7748 ms, echo time = 86 ms, flip angle = 90°, diffusion gradient (monopolar) directions = 64, diffusion gradient timing DELTA/delta = 42.4/10 ms, b-values: 0, 1000 s/mm^2, fat suppression using SPIR, field of view = 224 × 224 mm, in-plane resolution = 2 mm isotropic, number of transverse interleaved slices = 60, zero gap, slice thickness = 2 mm, SENSE factor = 2, and total acquisition time = 10 min 51 s.

Longitudinal free-water mapping analysis

Figure 1A depicts the general processing pipeline. Data preprocessing was performed with the FMRIB Software Library (FSL; Oxford, UK) and custom UNIX shell scripts. Each diffusion scan was corrected for distortions due to eddy currents and head motion using affine transformations. Motion was extracted from the affine motion and eddy current correction, and quantified by the root mean square deviation averaged over 64 volumes. The root mean square deviation is the average difference between the centre of volume of the b0 and each diffusion volume in millimetres. There were no baseline ($P = 0.88$) or Year 1 differences ($P = 0.58$) in motion between groups. The gradient directions were then rotated in response to the eddy current corrections, and non-brain tissue was removed from the diffusion volumes.

Free-water maps and free-water corrected diffusion tensor maps were calculated from the motion and eddy current corrected volumes using a custom written MATLAB R2013a (The Mathworks) code (Pasternak *et al.*, 2009, 2012). This code implemented a minimization procedure that fits a bi-tensor model, which quantifies the fractional volume of free-water in each voxel (free-water maps). The bi-tensor model predicts the signal attenuation in the presence of free-water contamination. It is the sum of attenuations contributed by two compartments: one that models free water, and a second tissue compartment that models water molecules in the vicinity of tissue membranes. The free-water maps are the fractional volume of the free-water compartment. The tissue compartment follows DTI's formalism (Basser and Pierpaoli, 1996), where the attenuation is parameterized by a diffusion tensor, yielding corrected DTI measures, such as fractional anisotropy (FA) of the tissue compartment (FA_T) and mean diffusivity (MD) of the tissue compartment (MD_T). Finding the free-water parameter and the corrected diffusion tensor that best fit the acquired signal is non-trivial and is described in detail in previous work (Pasternak *et al.*, 2009).

To obtain standardized space representation of diffusion images with consistent region of interest sizes across subjects for both visits, the free-water maps were warped using the deformation obtained from the registration of the individual's b-zero maps to a standardized T_2 image (Fonov *et al.*, 2011) in MNI space (2 × 2 × 2 mm). The linear registration was performed by an affine transformation with 12 degrees of freedom and tri-linear interpolation using FLIRT (http://fsl.fmrib.ox.ac.uk/fsl/fslwiki/FLIRT). The transformations were subsequently applied to the free-water, FA_T and MD_T maps.

Table 2 Patient medication

Drug	Brand names	Dosage range/use	Half-life range	Number of participants baseline	Number of participants Year 1
Carbidopa-Levodopa	Atamet® Sinamet®	25–100 mg	60 to 90 min	19	22
Pramipexole	Mirapex®	0.5–1.5 mg	8–12 h	6	8
Amantadine	Symmetrel®	100 mg	2–4 h	2	5
Ropinirole	Requip® Requip XL®	0.5–12 mg	6 h	2	3
Entacapone	Comtan®	200 mg	0.5–2.5 h	1	0
Apomorphine	Apokyn®	10 mg/3 ml	0.5 to 1 h	1	0
Rotigotine Transdermal Patch	Neupro®	2–6 mg patches	5–7 h	2	4
Selegiline	Zelepar®	5 mg	2–10 h	1	1

Regions of interest in the substantia nigra

Regions of interest were manually placed on the b0 image in MNI space separately for each visit and each subject. Regions of interest were hand-drawn by two trained raters, blinded to the free-water map and blinded to the group category and visit. After setting the regions of interest, free-water, FA_T, and MD_T were quantified within each region of interest in MNI space. Figure 1B shows a zoomed-in axial slice of the free-water image with the corresponding regions of interest for the substantia nigra, which was drawn based on previous work (Vaillancourt *et al.*, 2012). Each region of interest included 10 voxels that spanned two axial slices on each image. The dorsal slice contained a rectangular region of interest of six voxels (2 × 3) and the ventral region of interest consisted of a square region of interest of four voxels (2 × 2). Regions of interest were drawn on the left and right anterior and posterior regions of the substantia nigra. The posterior regions were mostly drawn in voxels lateral to the anterior regions of interest. Across subjects, the average centre of mass (COM) coordinates for the posterior substantia nigra were $x = -10.5$, $y = 20.8$ and $z = -12.8$ for the right substantia nigra region of interest and $x = 10.4$, $y = 20.6$, $z = -12.8$ for the left substantia nigra region of interest. The average centre of mass coordinates for the anterior substantia nigra were $x = -9.0$, $y = 15.5$ and $z = -12.8$ for the right substantia nigra region of interest and $x = 8.9$, $y = 15.3$, $z = -12.8$ for the left substantia nigra region of interest.

Control regions of interest

Control regions of interest were manually drawn on the b0 images in MNI space for each visit and each subject for the subthalamic nucleus and the lateral ventricles of each individual. The subthalamic nucleus was identified based on the Basal Ganglia Human Area Template (BGHAT) (Prodoehl *et al.*, 2008). The subthalamic nucleus was drawn bilaterally and comprised of 18 voxels. Across subjects, the average centre of mass coordinates were $x = -12.2$, $y = 13.6$ and $z = -6.5$ for the right subthalamic nucleus region of interest and $x = 11.8$, $y = 13.7$, $z = -6.5$ for the left subthalamic nucleus region of interest. The lateral ventricle region of interest was drawn medial to the caudate nuclei along the septum and inferior to the corpus callosum. This area was chosen as a high fluid-filled control region that displays a substantial amount of hyperintensity on the free-water maps. The region of interest was drawn bilaterally around the longitudinal fissure and comprised of 30 voxels. Across subjects, the average centre of mass coordinates were $x = 0$, $y = -14.3$ and $z = 4$.

T_1 MRI acquisition

To determine if changes in grey matter and white matter volumes occurred over time, we used a 3D fast gradient echo T_1-weighted sequence with the following parameters: repetition time = 8.2 ms, echo time = 3.7 ms, flip angle = 8°, field of view = 240 mm^2, acquisition matrix = 240 × 240, voxel size = 1 mm isotropic ($n = 170$, transverse), SENSE factor = 1.5, and total acquisition time = 7 min and 56 s.

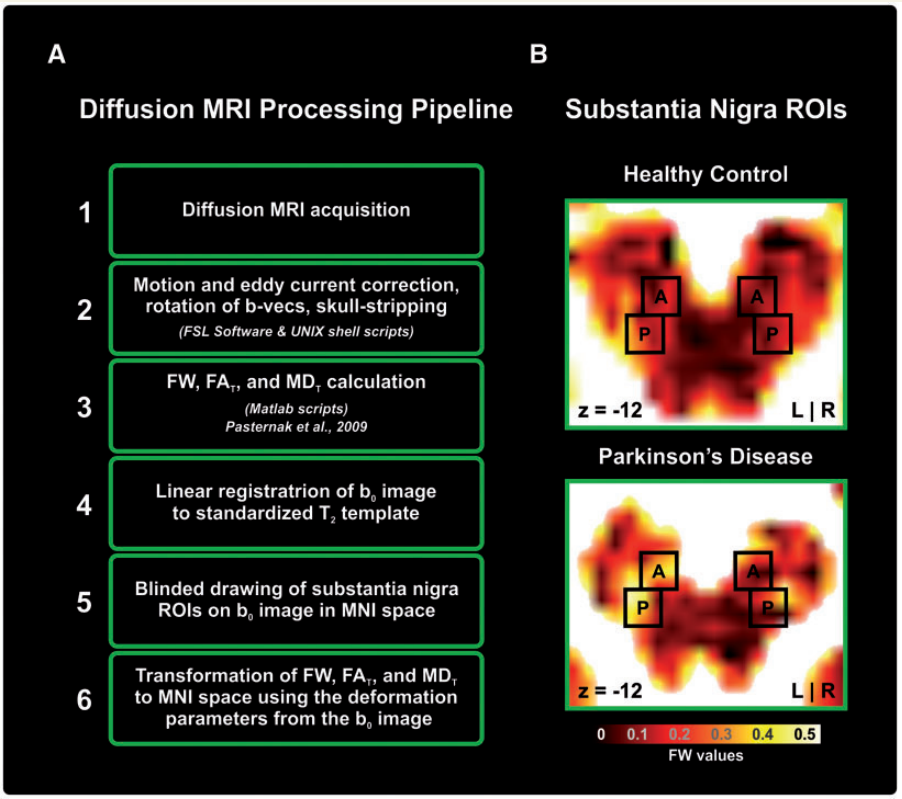

Figure 1 Processing pipeline and regions of interest. (**A**) A flow chart that indicates the steps of the diffusion MRI processing pipeline from acquisition to the calculation of diffusion indices. (**B**) A black-body radiation coloured free-water (FW) image of substantia nigra regions of interest (ROIs) for controls and Parkinson's disease.

Longitudinal voxel-based morphometry analysis

Data processing was performed using the VBM 8 toolbox (http://dbm.neuro.uni-jena.de/vbm/), incorporated in the SPM 8 software (htttp://www.fil.ion.ucl.ac.uk/spm/). The longitudinal preprocessing approach included the following steps: (i) T_1-weighted scans were coregistered to the white matter template supplied with SPM 8; (ii) registration of the scan from the second visit to the scan from the first visit for each patient separately; (iii) intra-subject bias corrections for signal inhomogeneities were performed; (iv) each scan was partitioned into grey matter, white matter and CSF; (v) a linear followed by a non-linear registration to the DARTEL template was performed; (vi) to correct for the local expansion or contraction inherent to the normalization process, grey matter and white matter images were non-linearly modulated using the Jacobian of the warp field, a step which also accounts for differences in brain size; and (vii) modulated normalized grey matter and white matter scans were smoothed with an 8-mm full-width at half-maximum Gaussian kernel.

Statistical analysis

Demographic and clinical data between groups were subjected to either repeated measures ANOVA or chi-square tests.

The mean values of the anterior and posterior substantia nigra and control regions of interest were calculated bilaterally for each dependent measure (free-water, FA_T, MD_T). The distributions of the dependent variables were tested using Shapiro-Wilk test for normality to verify that the sample mean is an appropriate measure. A repeated measures ANCOVA with sex as a covariate and time as a within-subject factor was conducted to detect group and time differences between patients with Parkinson's disease and healthy control subjects. Paired *t*-tests were used *post hoc* to examine any interaction effects. Inter-rater reliability of manual region of interest delineation was examined using intraclass correlation coefficients (ICC) between the two raters.

To assess whether the baseline free-water can aid in the prediction of change in clinical symptom assessment over 1 year, we used a forward selection linear regression model with baseline free-water and sex as independent variables for each dependent measure found to change significantly over 1 year (i.e. MDS-UPDRS III scores and bradykinesia sub-scores). Changes across time were calculated as 1 year values minus baseline values. We also used MoCA as a dependent measure as we have previously found that MoCA scores correlate with free-water values using cross-sectional data (Ofori *et al.*, 2015). To check for internal validity, we applied a 95% confidence interval (CI) bootstrapping procedure of 2000 samples with a bias-corrected CI type. All statistical analyses were performed with IBM SPSS Statistics 22 (SPSS, Inc, Chicago, IL). The significance threshold for all analyses was 0.05. *P*-values were corrected using the Benjamini-Hochberg false discovery rate (FDR) method for multiple comparisons (Benjamini and Hochberg, 1995). FDR corrected *P*-values are reported for all substantia nigra diffusion dependent measures.

A voxel-wise paired *t*-test was performed on the voxel-based morphometry analysis to examine differences between the baseline and 1 year visits. To reduce the risk of type 1 errors in the voxel-based morphometry analysis, *P*-values were corrected using the familywise error rate (FWE) method for multiple comparisons. Exploratory uncorrected *P*-values were also examined.

Results

Demographic and clinical information

Table 1 shows the demographic and clinical characteristics of healthy controls and patients with Parkinson's disease at baseline and 1 year. There were no group differences in age and hand dominance, and sex approached significance. The Parkinson's disease group had higher MDS-UPDRS III total and sub-scores ($P < 0.001$), higher Beck Depression Inventory ($P = 0.012$), and lower MoCA ($P = 0.023$) scores when compared with healthy controls. A time effect ($P = 0.007$) was found for the MDS-UPDRS III and a group × time interaction ($P = 0.05$) was found for the bradykinesia subscore. The interaction resulted in a greater change in bradykinesia for Parkinson's disease (mean = 3.4, $P = 0.001$) than in controls (mean = 1.2, $P = 0.015$). There were no other significant changes in any other clinical or demographic data over time (Table 1).

Substantia nigra regions of interest

Posterior regions of interest

Figure 2 illustrates the group, time, and group × time interaction of mean free-water in the posterior substantia nigra for Parkinson's disease and healthy controls. The group effect resulted in greater mean free-water for Parkinson's

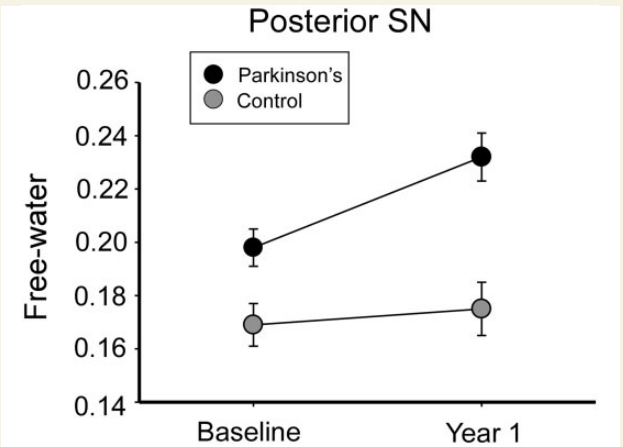

Figure 2 Free-water content of the posterior substantia nigra for controls and Parkinson's disease. The mean free-water content of the posterior substantia nigra (SN) for healthy controls and Parkinson's patients at baseline and Year 1. Error bars are ±1 standard error of mean.

Table 3 Substantia nigra region of interest analysis results for diffusion metrics

	Healthy controls ($n = 19$)		Parkinson's patients ($n = 25$)				
	Baseline	Year 1	Baseline	Year 1	Group effect	Time effect	Interaction
Posterior SN free-water	0.172 (0.01)	0.173 (0.01)	0.195 (0.01)	0.233 (0.01)	0.004**	0.03**	0.0495*
Posterior SN FA_T	0.609 (0.01)	0.592 (0.01)	0.626 (0.01)	0.629 (0.01)	0.09	0.955	0.467
Posterior SN MD_T	0.550 (0.01)	0.507 (0.01)	0.564 (0.01)	0.564 (0.005)	0.787	0.955	0.322
Anterior SN free-water	0.184 (0.01)	0.214 (0.01)	0.197 (0.01)	0.23 (0.01)	0.322	0.090	0.945
Anterior SN FA_T	0.607 (0.02)	0.639 (0.01)	0.625 (0.01)	0.696 (0.01)	0.090	0.036*	0.110
Anterior SN MD_T	0.540 (0.007)	0.559 (0.01)	0.547 (0.01)	0.558 (0.01)	0.787	0.142	0.467

*$P < 0.05$, **$P < 0.01$, Values in parentheses are standard error of mean; P-values are FDR corrected.

disease compared with controls ($P = 0.003$). The group-time interaction ($P < 0.05$) identified an increased mean free-water for Parkinson's disease over time ($P = 0.006$), whereas there were no significant differences between baseline and 1 year values for controls ($P = 0.483$). There were no significant effects for MD_T and FA_T across group, time, or group × time interactions ($P > 0.05$) (Table 3).

Anterior region of interest

There were no significant differences in group, time, or group × time interactions for free-water in the anterior substantia nigra for Parkinson's disease and healthy controls ($P > 0.05$). There was a time effect ($P < 0.05$) for FA_T in the anterior substantia nigra, identifying an increase in FA_T over 1 year across groups. There were no group effects or group × time interactions for FA_T in the anterior substantia nigra ($P > 0.05$). There were no effects of group, time, or group × time interaction for MD_T in the anterior substantia nigra of Parkinson's disease and healthy controls (Table 3).

Inter-rater reliability

The ICC was high for all of the substantia nigra regions of interest. We found an ICC of 0.92 for the left anterior substantia nigra region of interest, 0.90 for the right anterior substantia nigra region of interest, 0.89 for the left posterior region of interest, and 0.86 for the right posterior substantia nigra region of interest. We performed paired t-tests between mean free-water values in each region of interest drawn by the two raters, which did not identify any significant differences between raters ($P > 0.40$).

Control regions of interest

There were no significant group, time, or interaction effects for the lateral ventricle region of interest and subthalamic nucleus free-water, FA_T, and MD_T values (P's > 0.05).

Free-water at baseline predicts the 1-year change in clinical bradykinesia

Figure 3A shows the linear relation between baseline free-water values of the posterior substantia nigra, sex, and actual change in bradykinesia over 1 year. The linear regression model indicated that baseline free-water values ($B_1 = 73.38$, $P < 0.001$) and sex ($B_2 = -6.7$, $P < 0.001$) significantly predicted the change in bradykinesia of Parkinson's disease ($r = 0.74$, $P < 0.001$; $n = 25$) (Fig. 3B). The bootstrap estimates and confidence intervals for baseline free-water values ($B_1 = 73.38$, $P = 0.001$; CI = 50.73 to 123.26; bias = 3.04) and sex ($B_2 = -6.7$, $P = 0.001$; CI = −8.97 to −4.63; bias = −0.04) were significant for the prediction of change in bradykinesia. The model for controls was not significant ($r = 0.30$, $P = 0.47$; $n = 19$). Figure 3C and D show that the baseline free-water values significantly predict the change in MoCA ($r = -0.44$, $P < 0.03$; $n = 25$) for Parkinson's disease. The bootstrap estimates and CI's for baseline free-water values ($B_3 = -28.9$, $P = 0.04$; CI = −59.0 to −7.2; bias = −1.82) were significant for the prediction of MoCA. This was not found for controls ($r = 0.22$, $P = 0.67$; $n = 19$).

Longitudinal voxel-based morphometry

There were no significant differences in total grey matter and total white matter volumes between Parkinson's disease and controls at baseline, or between baseline and 1 year follow-up in either Parkinson's disease or controls. Relaxing the P-value to uncorrected $P < 0.05$ did not reveal any changes in the substantia nigra.

Discussion

Non-invasive diffusion MRI markers of substantia nigra integrity have aided in characterizing Parkinson's disease within substantia nigra microstructure. Previous studies in Parkinson's disease have demonstrated that diffusion MRI is sensitive to substantia nigra changes even in the *de novo* Parkinson's disease stage, suggesting that these observations are not secondary to drug effects (Vaillancourt *et al.*, 2009; Ofori *et al.*, 2015). The current longitudinal study provides novel evidence that: (i) diffusion MRI of the substantia nigra is capable of detecting progression after 1 year; and (ii) baseline free-water levels predict the subsequent increase in bradykinesia the following year.

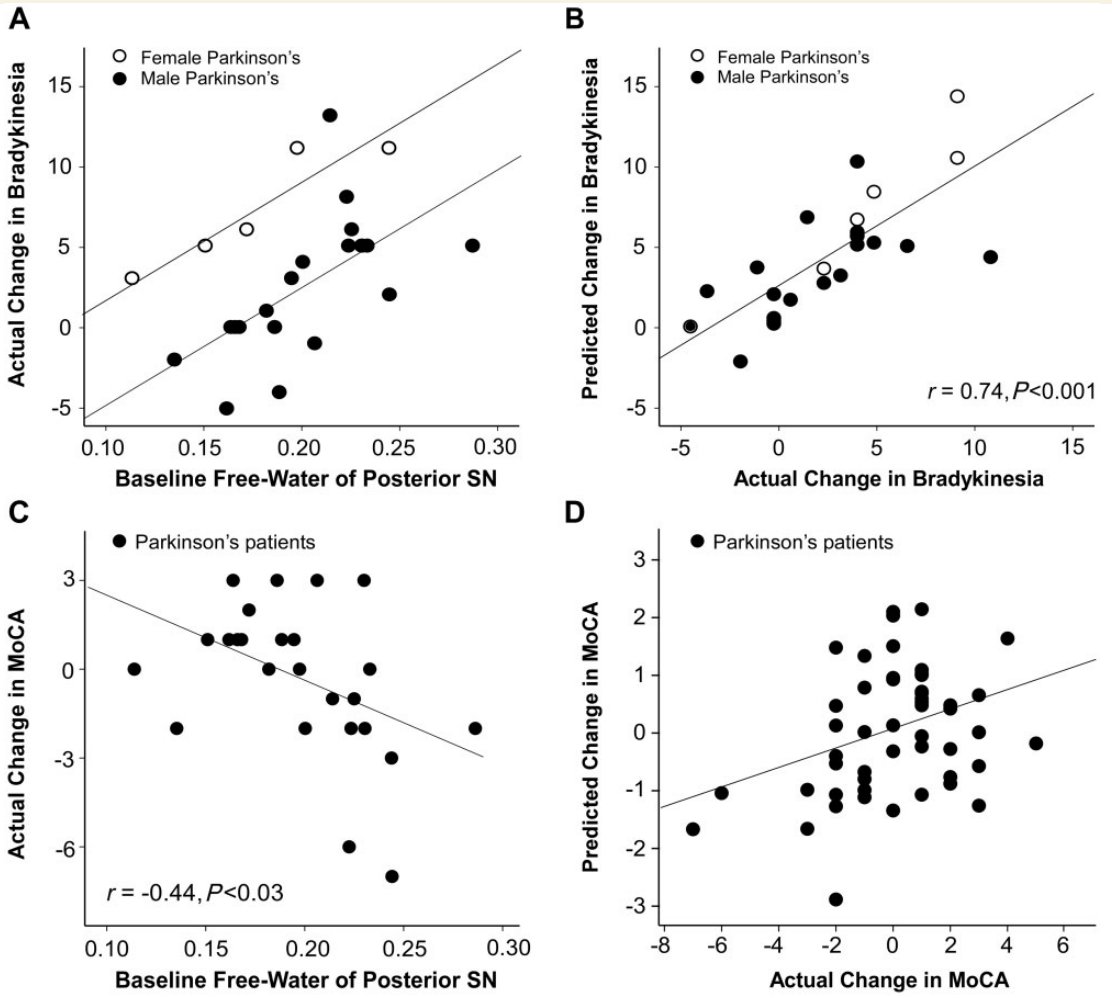

Figure 3 Free-water content and change in clinical symptoms. (**A**) Scatterplot with actual change in bradykinesia along regression lines of the predicted change in bradykinesia over 1 year across males and females as a function of baseline free-water values. (**B**) Scatterplot of predicted change in bradykinesia and actual change in bradykinesia for patients with Parkinson's disease. (**C**) Scatterplot of baseline free-water values and change in MoCA. (**D**) Scatterplot of predicted change in MoCA and actual change in MoCA for patients with Parkinson's disease. SN = substantia nigra.

Brain cells change their shape during osmotic challenges (i.e. relative water accumulation) imposed by the extracellular space (Chen and Nicholson, 2000). Recent work using 7 T MRI and 3D shape analysis demonstrated increased irregularity in the dorsomedial and caudal boundaries of the substantia nigra in patients with Parkinson's disease when compared with control subjects (Kwon *et al.*, 2012). Kwon and colleagues (2012) inferred changes in the relative structural shape of the substantia nigra with iron accumulation. These proposed cellular alterations would change substantia nigra cellularity and in turn increase the fluid content in the local area. Consistent with this hypothesis, our findings demonstrated high free-water levels within the posterior substantia nigra in Parkinson's disease, levels that further increased following 1 year of progression in the same cohort. Posterior substantia nigra free-water levels did not change over 1 year in the control group, suggesting that elevation in free-water levels was specific to Parkinson's disease. It is, however, possible that age-effects would be detected over a longer time-scale (Sexton *et al.*, 2014).

Dopaminergic cell loss of the substantia nigra in patients with Parkinson's disease has been shown to be greatest in the ventrolaterior tier of the substantia nigra pars compacta (SNc) and progress to other areas of the substantia nigra (Fearnley and Lees, 1991; Kordower *et al.*, 2013). Recently, a pathological study attributed increased dopaminergic dysfunction of the SNc with disease duration (Kordower *et al.*, 2013). The authors demonstrated that the number of tyrosine-hydroxylase-immunoreactivity cells decreased even in a patient with 1 year of disease duration and remained decreased across different disease durations (Kordower *et al.*, 2013). The spatial pattern of the current findings that indicated an increase in free-water over 1 year might possibly be related to the degeneration of dopaminergic cells in Parkinson's disease over time, given that previous studies have found a link between the number of

dopaminergic cells and diffusion measurements in a parkinsonian mouse model (Boska *et al.*, 2007).

Another important feature is the breakdown in dopamine active transporter (DAT) function, which is well documented in Parkinson's disease (Marek *et al.*, 2001; Jennings *et al.*, 2004). We previously found an inverse relation between DAT-SPECT from the putamen and the free-water levels in the substantia nigra (Ofori *et al.*, 2015), suggesting that impaired DAT function may be related to increased free-water in the substantia nigra. The current findings support the interpretation that posterior substantia nigra free-water values provide a marker for the relative state of the substantia nigra. It should be noted that motor symptom deficits have been shown to occur in Parkinson's disease when ~50% of the region is depleted. Our results demonstrating an increase of free-water over time in Parkinson's disease could inversely relate to the functional status of surviving dopaminergic nerve terminals. This could explain the correlation between baseline free-water values and longitudinal change in bradykinesia scores. Further work is needed on the relationship between DAT binding values, dopaminergic cells, and free-water values of the nigrostriatal system.

Although previous studies have reported reduced fractional anisotropy in the substantia nigra (Vaillancourt *et al.*, 2009; Péran *et al.*, 2010; Du *et al.*, 2011), other studies have not found this result (Schwarz *et al.*, 2013; Ziegler *et al.*, 2014). One reason for this discrepancy in the literature is that free-water contamination can lead to reduced fractional anisotropy values (Metzler-Baddeley *et al.*, 2012). It has also been reported that fractional anisotropy values may increase when using diffusion kurtosis imaging (Wang *et al.*, 2011*a*). Due to the inconsistent fractional anisotropy findings across previous studies, a recent meta-analysis (Schwarz *et al.*, 2013) indicates that fractional anisotropy may not differ in Parkinson's disease compared with controls. Our current data support the suggestion that FA_T does not differ between Parkinson's disease and controls. As the bi-tensor model is able to disentangle free-water contamination leading to decreased fractional anisotropy from tissue changes that may lead to increased fractional anisotropy, the current study suggests that using free-water correction could be particularly helpful in detecting changes in the substantia nigra of Parkinson's disease. Evidence of the importance of quantifying free-water using the bi-tensor model rather than the classic diffusion tensor imaging model was provided by Ofori and colleagues (2015), which showed that free-water was elevated in the same posterior substantia nigra region in single site at an academic centre and multi-site cohorts from the Parkinson's Progression Marker Initiative. In this prior study, FA_T was not different between groups in either cohort, further emphasizing the need for more advanced analysis methods beyond the classic diffusion tensor imaging model.

Although free-water corrected fractional anisotropy did not differ between patients with Parkinson's disease and healthy controls in the current study, free-water corrected fractional anisotropy in the anterior substantia nigra was found to increase over 1 year. Previous studies have examined longitudinal effects on diffusion metrics of healthy controls and found that fractional anisotropy changes may be attributed to gliosis/glial cell swelling or local fibre activity (Madden *et al.*, 2012), and this may be due to altered shape of the extracellular space (Mandl *et al.*, 2008; Pasternak *et al.*, 2009). Gliosis has also been suggested to be a compensatory mechanism for deficits in dopamine function in Parkinson's disease (Sanchez-Guajardo *et al.*, 2013). Further work is needed on the relationship between the role of gliosis in the substantia nigra, free-water and its role on dopamine function in Parkinson's disease. The increase over a year in control subjects and patients with Parkinson's disease could be due to age-related effects that naturally occur in the substantia nigra over time (Fearnley and Lees, 1991). Previous work from our laboratory has shown altered fractional anisotropy values in anterior but not posterior substantia nigra regions of interest in a cross-sectional study on healthy ageing (Vaillancourt *et al.*, 2012). Although the causal mechanism for the increase in fractional anisotropy is hard to discern from the current data, it is interesting to note that the controls and patients with Parkinson's disease MDS-UPDRS-III scores increased over a year.

There is an increasing need for non-invasive Parkinson's disease markers that can detect progressing changes in the substantia nigra. Cross-sectional analysis of the R^{2*} technique has found a relationship between R^{2*} values in the substantia nigra and disease severity, as measured by the UDPRS (Martin *et al.*, 2008). Longitudinal studies using R^{2*} imaging have shown a positive association between the change of signal values in the substantia nigra for Parkinson's disease and change in disease severity over 3 years (Ulla *et al.*, 2013). Ulla and colleagues (2013) noted that a large amount of R^{2*} was non-iron dependent and sensitive to the neurodegenerative processes that altered the water content. The current paper extends this previous work by showing that baseline free-water values from diffusion MRI predicted subsequent changes in bradykinesia and MoCA in patients with Parkinson's disease over 1 year of follow-up. Future studies will likely establish if R^{2*} imaging of the substantia nigra reflects changes after 1 year of disease progression. Prior studies comparing diffusion tensor imaging and R^{2*} measures have not found a significant relation between these two techniques (Péran *et al.*, 2010; Du *et al.*, 2011), although newer studies point to a relationship between R^{2*} and diffusion metrics when monopolar diffusion gradients are applied (Fujiwara *et al.*, 2014). In our case the diffusion sequence used monopolar gradients, and therefore some of the free-water changes may be explained by R^{2*} changes. Fujiwara and colleagues (2014) found that increased iron content would decrease mean diffusivity, and thus is also expected to decrease free-water. However, in our data we observe an opposite finding of increased free-water in Parkinson's

disease, suggesting that increased iron content is not likely the cause for this change. The free-water parameter is also affected by changes in the T_2 or in the T_1 of the free-water and tissue compartments (Pasternak *et al.*, 2009). We note, however, that increased water content would similarly affect T_2 and free-water (i.e. both would increase) (Pasternak *et al.*, 2012). Additional separation between the effects caused by increased extracellular space, and changes that affect T_1, T_2 or the magnetic field inhomogeneity require bipolar diffusion acquisition, and additional multi-echo T_1 and T_2 acquisition sequences. Nonetheless, the current finding between change in bradykinesia and cognitive status and baseline free-water values provides new evidence that non-invasive diffusion MRI may be a progression marker of Parkinson's disease.

The findings from the current study reveal an increase in free-water values evolving over 1 year in a well-characterized Parkinson's disease cohort. We present new findings that free-water values of the substantia nigra could potentially provide a marker of progression in Parkinson's disease, and predict clinical bradykinesia and MoCA in the subsequent year of follow-up. Free-water values may provide a window into the degree of substantia nigra integrity and could serve as a marker of substantia nigra degeneration in therapeutic trials aimed at slowing substantia nigra degeneration in Parkinson's disease.

Acknowledgements

The authors would like to thank the participants and their families for their time and commitment to this research.

Funding

This work was supported by the National Institutes of Health (R01 NS052318, R01 NS075012) and the Bachmann-Strauss Dystonia and Parkinson Foundation. MRI data collection was supported through the Human Imaging Core of the University of Florida Clinical and Translational Science Institute (UL1 TR000064) through the National Institutes of Health's Clinical and Translational Science Awards program, and the National High Magnetic Field Laboratory at the Advanced Magnetic Resonance Imaging and Spectroscopy.

References

Basser PJ, Pierpaoli C. Microstructural and physiological features of tissues elucidated by quantitative-diffusion-tensor MRI. J Magn Reson B 1996; 111: 209–19.

Beck AT, Ward CH, Mendelson M, Mock J, Erbaugh J. An inventory for measuring depression. Arch Gen Psychiatry 1961; 4: 561–71.

Benjamini Y, Hochberg Y. Controlling the false discovery rate: a practical and powerful approach to multiple testing. J R Stat Soc B 1995; 57: 289–300.

Boska MD, Hasan KM, Kibuule D, Banerjee R, McIntyre E, Nelson JA, et al. Quantitative diffusion tensor imaging detects dopaminergic neuronal degeneration in a murine model of Parkinson's disease. Neurobiol Dis 2007; 26: 590–6.

Chen KC, Nicholson C. Changes in brain cell shape create residual extracellular space volume and explain tortuosity behavior during osmotic challenge. Proc Natl Acad Sci USA 2000; 97: 8306–11.

Damier P, Hirsch EC, Agid Y, Graybiel AM. The substantia nigra of the human brain. II. Patterns of loss of dopamine-containing neurons in Parkinson's disease. Brain 1999; 122 (Pt 8): 1437–48.

Du G, Lewis MM, Styner M, Shaffer ML, Sen S, Yang QX, et al. Combined R2* and diffusion tensor imaging changes in the substantia nigra in Parkinson's disease. Mov Disord 2011; 26: 1627–32.

Fearnley JM, Lees AJ. Ageing and Parkinson's disease: substantia nigra regional selectivity. Brain 1991; 114: 2283–301.

Fonov V, Evans AC, Botteron K, Almli CR, McKinstry RC, Collins DL. Unbiased average age-appropriate atlases for pediatric studies. Neuroimage 2011; 54: 313–27.

Fujiwara S, Uhrig L, Amadon A, Jarraya B, Le Bihan D. Quantification of iron in the non-human primate brain with diffusion-weighted magnetic resonance imaging. Neuroimage 2014; 102 (Pt 2): 789–97.

Goetz CG, Stebbins GT, Tilley BC. Calibration of unified Parkinson's disease rating scale scores to Movement Disorder Society-unified Parkinson's disease rating scale scores. Mov Disord 2012; 27: 1239–42.

Hughes AJ, Ben-Shlomo Y, Daniel SE, Lees AJ. What features improve the accuracy of clinical diagnosis in Parkinson's disease: a clinicopathologic study 1992. Neurology 2001; 57: S34–8.

Jennings DL, Seibyl JP, Oakes D, Eberly S, Murphy J, Marek K. (123I) beta-CIT and single-photon emission computed tomographic imaging vs clinical evaluation in Parkinsonian syndrome: unmasking an early diagnosis. Arch Neurol 2004; 61: 1224–9.

Kordower JH, Olanow CW, Dodiya HB, Chu Y, Beach TG, Adler CH, et al. Disease duration and the integrity of the nigrostriatal system in Parkinson's disease. Brain 2013; 136: 2419–31.

Kwon DH, Kim JM, Oh SH, Jeong HJ, Park SY, Oh ES, et al. Seven-tesla magnetic resonance images of the substantia nigra in Parkinson disease. Ann Neurol 2012; 71: 267–77.

Madden DJ, Bennett IJ, Burzynska A, Potter GG, Chen N, Song AW. Diffusion tensor imaging of cerebral white matter integrity in cognitive aging. Biochim Biophys Acta 2012; 1822: 386–400.

Mandl RCW, Schnack HG, Zwiers MP, van der Schaaf A, Kahn RS, Hulshoff Pol HE. Functional diffusion tensor imaging: measuring task-related fractional anisotropy changes in the human brain along white matter tracts. PLoS One 2008; 3: e3631.

Marek K, Innis R, van Dyck C, Fussell B, Early M, Eberly S, et al. [123I]beta-CIT SPECT imaging assessment of the rate of Parkinson's disease progression. Neurology 2001; 57: 2089–94.

Martin WR, Wieler M, Gee M. Midbrain iron content in early Parkinson disease: a potential biomarker of disease status. Neurology 2008; 70: 1411–7.

Metzler-Baddeley C, O'Sullivan MJ, Bells S, Pasternak O, Jones DK. How and how not to correct for CSF-contamination in diffusion MRI. Neuroimage 2012; 59: 1394–403.

Ofori E, Pasternak O, Planetta PJ, Burciu R, Snyder A, Febo M, et al. Increased free water in the substantia nigra of Parkinson's disease: a single-site and multi-site study. Neurobiol Aging 2015; 36: 1097–104.

Pasternak O, Sochen N, Gur Y, Intrator N, Assaf Y. Free water elimination and mapping from diffusion MRI. Magn Reson Med 2009; 62: 717–30.

Pasternak O, Westin CF, Bouix S, Seidman LJ, Goldstein JM, Woo TUW, et al. Excessive extracellular volume reveals a neurodegenerative pattern in schizophrenia onset. J Neurosci 2012; 32: 17365–72.

Péran P, Cherubini A, Assogna F, Piras F, Quattrocchi C, Peppe A, et al. Magnetic resonance imaging markers of Parkinson's disease nigrostriatal signature. Brain 2010; 133: 3423–33.

Prodoehl J, Yu H, Little DM, Abraham I, Vaillancourt DE. Region of interest template for the human basal ganglia: comparing EPI and standardized space approaches. Neuroimage 2008; 39: 956–65.

Prodoehl J, Spraker M, Corcos D, Comella C, Vaillancourt D. Blood oxygenation level-dependent activation in basal ganglia nuclei relates to specific symptoms in de novo Parkinson's disease. Mov Disord 2010; 25: 2035–43.

Prodoehl J, Li H, Planetta PJ, Goetz CG, Shannon KM, Tangonan R, et al. Diffusion tensor imaging of Parkinson's disease, atypical parkinsonism, and essential tremor. Mov Disord 2013; 28: 1816–22.

Rossi ME, Ruottinen H, Saunamaki T, Elovaara I, Dastidar P. Imaging brain iron and diffusion patterns: a follow-up study of Parkinson's disease in the initial stages. Acad Radiol 2014; 21: 64–71.

Sanchez-Guajardo V, Barnum CJ, Tansey MG, Romero-Ramos M. Neuroimmunological processes in Parkinson's disease and their relation to α-synuclein: microglia as the referee between neuronal processes and peripheral immunity. ASN Neuro 2013; 5: 113–39.

Schwarz ST, Abaei M, Gontu V, Morgan PS, Bajaj N, Auer DP. Diffusion tensor imaging of nigral degeneration in Parkinson's disease: a region-of-interest and voxel-based study at 3 T and systematic review with meta-analysis. Neuroimage Clin 2013; 3: 481–8.

Sexton CE, Walhovd KB, Storsve AB, Tamnes CK, Westlye LT, Johansen-Berg H, et al. Accelerated changes in white matter microstructure during aging: a longitudinal diffusion tensor imaging study. J Neurosci 2014; 34: 15425–36.

Ulla M, Bonny JM, Ouchchane L, Rieu I, Claise B, Durif F. Is R2* a new MRI biomarker for the progression of Parkinson's disease? A longitudinal follow-up. PLoS One 2013; 8: e57904.

Vaillancourt DE, Spraker MB, Prodoehl J, Abraham I, Corcos DM, Zhou XJ, et al.. High-resolution diffusion tensor imaging in the substantia nigra of *de novo* Parkinson disease. Neurology 2009; 72: 1378–84.

Vaillancourt DE, Spraker MB, Prodoehl J, Zhou XJ, Little DM. Effects of aging on the ventral and dorsal substantia nigra using diffusion tensor imaging. Neurobiol Aging 2012; 33: 35–42.

Wang JJ, Lin WY, Lu CS, Weng YH, Ng SH, Wang CH, et al. Parkinson disease: diagnostic utility of diffusion kurtosis imaging. Radiology 2011a; 261: 210–17.

Wang Y, Wang Q, Haldar JP, Yeh FC, Xie M, Sun P, et al. Quantification of increased cellularity during inflammatory demyelination. Brain 2011b; 134: 3590–601.

Ziegler E, Rouillard M, Andre E, Coolen T, Stender J, Balteau E, et al. Mapping track density changes in nigrostriatal and extranigral pathways in Parkinson's disease. Neuroimage 2014; 99: 498–508.